Title: Direct labeling of polyphosphate at the ultrastructural level in *Saccharomyces cerevisiae* using affinity of the polyphosphate binding domain of *Escherichia coli* exopolyphosphatase

Running title: Direct labeling of polyphosphate in yeast

Authors: KATSUHARU SAITO,[1]† RYO OHTOMO,[1] YUKARI KUGA-UETAKE,[2] TOSHIHIRO AONO,[3] and MASANORI SAITO[4]*

Department of Grassland Ecology, National Institute of Livestock and Grassland Science, 768 Senbonmatsu, Nishinasuno, Tochigi 329−2793, Japan;[1] Department of Food Production Science, Faculty of Agriculture, Shinshu University, 8304 Minami-minowa, Kami-ina, Nagano 399–4598, Japan;[2] Department of Biotechnology, Graduate School of Agricultural and Life Sciences, University of Tokyo, 1–1–1 Yayoi, Bunkyo-ku, Tokyo, 113–8657, Japan;[3] and Department of Environmental Chemistry, National Institute for Agro-Environmental Sciences, 3−1−3 Kannondai, Tsukuba, Ibaraki 305−8604, Japan[4]

* Corresponding author. Mailing address: Department of Environmental Chemistry, National Institute for Agro-Environmental Sciences, 3–1–3 Kannondai, Tsukuba, Ibaraki 305–8604, Japan. Phone/Fax: 81 298 38 8300. E-mail: msaito@affrc.go.jp.
† Present address: CREST, Japan Science and Technology Corporation, Kawaguchi, Saitama 332–0012, Japan, and Graduate School of Science, University of Tokyo, Hongo, Bunkyo-ku, Tokyo 113–0033, Japan.

Abstract

Inorganic polyphosphate (poly P) is a linear polymer of orthophosphate and has many biological functions in prokaryotic and eukaryotic organisms. To investigate poly P localization, we developed a novel technique using the affinity of the recombinant polyphosphate binding domain (PPBD) of *Escherichia coli* exopolyphosphatase to poly P. An epitope-tagged PPBD was expressed and purified from *E. coli*. Equilibrium-binding assay of PPBD revealed its high affinity for long-chain poly P and its weak affinity for short-chain poly P and nucleic acids. To directly demonstrate poly P localization in *Saccharomyces cerevisiae* on resin sections prepared by rapid-freeze and freeze-substitution, specimens were labeled with PPBD containing an epitope tag, and then the epitope tag was detected by an indirect immunocytochemical method. A goat anti-mouse IgG antibody conjugated with Alexa 488 for laser confocal microscopy or with colloidal gold for transmission electron microscopy was used. When the *S. cerevisiae* was cultured in YPD medium (10 mM phosphate) for 10 hours, poly P was distributed in a dispersed fashion in vacuoles in successfully cryofixed cells. A few poly P signals of the labeling were sometimes observed in cytosol around vacuoles with electron microscopy. Under our experimental conditions, poly P granules were not observed. Therefore, it remains unclear whether the method can detect the granule form. The method directly demonstrated the localization of poly P at the electron microscopic level for the first time and enabled the visualization of poly P localization with much higher specificity and resolution than with other conventional methods.

Introduction

Inorganic polyphosphate (poly P) is a linear polymer of orthophosphate (Pi) connected by high-energy bonds. Poly P occurs in a wide range of organisms, including prokaryotes and eukaryotes. Poly P has various biological functions: for example, it acts as a Pi reservoir, as an alternative source of high-energy bonds, and as a buffer against alkaline conditions and metals (25). Furthermore, poly P also has regulatory functions such as competence for transformation (18), motility (36, 37), gene expression under stressed conditions (24, 35, 46) and protein degradation in amino acid starvation (28, 29) in prokaryotic organisms. The regulatory functions of poly P in eukaryotes are less clear, but some important facts are known. Recently, involvement of poly P in apoptosis (43) and enhancement of the mitogenic activities of acidic and basic fibroblast growth factors by poly P (45) have been suggested in mammalian cells.

The presence of poly P in cells can be visualized by staining with toluidine blue O (TBO) or 4′,6-diamidino-2-phenylindole (DAPI). DAPI is usually used for DNA detection, because blue fluorescence is apparent when the stained tissues are viewed under UV light. However, DAPI – poly P fluoresces yellow at high concentrations when viewed under UV (48). These staining methods have often been used for detecting poly P-accumulating bacteria in activated sludge (38, 44, 47) and poly P accumulation in the hyphae of arbuscular mycorrhizal fungi (12). Also, subcellular localization of poly P has been investigated using both TBO and DAPI staining. Bacterial poly P is found in cellular inclusions, known as metachromatic granules or volutin granules (26). In eukaryotic organisms, poly P has been shown to be localized in vacuoles (2), on the cell surfaces of yeasts (48), and in acidocalcisomes (30, 39, 41, 42), which are storage organelles for poly P and Ca^{2+} in protozoa and algae. TBO and DAPI are good probes for detecting cellular poly P easily, but it is sometimes difficult to determine the signals derived from poly P-bound probes, and the probes are not suitable for use in the ultrastructural analysis of poly P localization.

At the ultrastructural level, poly P appears as electron-dense regions, or the strong phosphorus signal of poly P is detected by electron microscopy coupled with energy

dispersive X-ray spectroscopy (EDXS) and electron energy loss spectroscopy (EELS). Phosphorus localization at the ultrastructural level has been investigated intensively by EDXS in ectomycorrhizal fungi, which are symbiotic organisms with plant roots that contribute to the improvement of plant nutrition (3, 4, 20). Formerly, on the basis of EDXS (6) and TBO staining (5), the poly P of ectomycorrhizal fungi was thought to be present as precipitated granules in vacuoles. However, poly P granules have been shown to be artifacts caused by ethanol dehydration following chemical fixation and by staining with cationic TBO (33). According to the results of EDXS analysis of freeze-substituted fungal hyphae, phosphorus in the vacuoles is not precipitated but is evenly dispersed, indicating that poly P is distributed in a soluble form in the vacuoles of living hyphae (7, 20, 33). However, poly P granules have been observed in non-fixed and air-dried algal cells (9) and in cryofixed and freeze-dried hyphae of ectomycorrhizal fungi (17). EELS is more advantageous for detecting light elements (e.g., phosphorus and nitrogen) and for spatial resolution than EDXS and has been used for P detection in poly P granules (13, 16, 22, 52). EELS can provide information on chemical bonding and the electronic states of compounds. However, it has not yet been used in such studies.

Here we developed a new technique to directly demonstrate poly P localization with high sensitivity and resolution by using the affinity of *Escherichia coli* exopolyphosphatase (PPX) for poly P. PPX is an enzyme that hydrolyzes the terminal phosphate bonds of poly P and consists of two domains: an N-terminal domain containing the PPX catalytic site and a C-terminal domain containing the poly P binding site (14, 15). In our procedure, poly P in thin sections of quick-frozen and freeze-substituted specimens was labeled with recombinant polyphosphate binding domain (PPBD) of PPX, containing an epitope tag at the N-terminal end, and then the epitope tag was detected by an indirect immunocytochemical method (Fig. 1B). We evaluated the binding specificity of PPBD to poly P and demonstrated poly P localization in *Saccharomyces cerevisiae* by this PPBD affinity procedure.

Materials and Methods

Strain and culture. *Saccharomyces cerevisiae* BY4741 (*MAT*a *his3*, *leu2*, *met15*, *ura3*) was purchased from the American Type Culture Collection (ATCC, Manassas, Va.). The yeast strain was grown at 30°C for 10 h in Pi-depleted YPD medium supplemented with either 0.2 mM (YPD-low Pi) or 10 mM (YPD-high Pi) potassium phosphate. Pi-depleted YPD was prepared as described (23, 40).

Purification of PPBD in PPX. Recombinant PPBD in PPX was prepared as described by Bolesch and Keasling (15), with the following modifications. The gene for the C-terminal PPBD of PPX (from glutamate 305) was amplified from the *E. coli* TOP10 f′ genome using PCR. Primers were 5′-CTGCAGAAATGGAAGGACGTTTCCGT-3′ and 5′-GAATTCCCCGCAAAGTATTAAGCGG-3′. The DNA amplified using these primers was first inserted into pGEM-T (Promega, Madison, Wisc.), creating pGEM-PPBD. The gene from pGEM-PPBD was then inserted into pTrc-HisB (Invitrogen, Carlsbad, Calif.), from *Pst*I (5′) to *Eco*RI (3′), yielding pTrc-PPBD. *E. coli* TOP10 f′ harboring pTrc-PPBD was cultured in 50 ml SOB with 50 μg ml^{-1} ampicillin at 37°C. The culture was induced with 1 mM isopropylthio-β-D-galactoside (IPTG) at an A_{600} of 0.6. After incubation for 2 h, cells were harvested by centrifugation and resuspended in 10 ml binding buffer (10 mM HEPES-KOH [pH 7.6], 0.1 M NaCl, 5 mM $MgCl_2$, 0.05 mM EDTA, 2 mM β-mercaptoethanol, 10% glycerol). Cells were lysed six times using a sonicator with a 10-s pulse and centrifuged at 20,000 × *g* for 10 min at 4°C. The supernatant was filtered through a 0.2-μm cellulose acetate membrane filter (Advantec, Tokyo, Japan) and loaded on a 5-ml Ni^{2+}-charged HiTrap Chelating HP column (Amersham, Piscataway, N.J.), pre-equilibrated with binding buffer, at a 2.5-ml min^{-1} flow rate using an FPLC system (Amersham). The column was washed with 50 ml washing buffer (10 mM HEPES-KOH [pH 7.6], 0.5 M NaCl, 5 mM $MgCl_2$, 0.05 mM EDTA, 2 mM β-mercaptoethanol, 10% glycerol). Recombinant protein was eluted with a linear imidazole gradient (0 to 0.5 M) in the binding buffer. The buffer was changed to 50 mM Tris-HCl (pH 9.0) using a PD-10 column (Amersham). An equal volume of glycerol was added to the purified protein, which was kept at –30°C for further use. Protein concentrations were measured by Bio-Rad Protein

Assay (Bio-Rad, Hercules, Calif.) with a bovine serum albumin (BSA) standard. SDS-PAGE and staining by Coomassie Brilliant Blue R-250 were performed, using size standards from Amersham.

Poly P binding assay for PPBD. [^{32}P]poly P was prepared as described by Kornberg and co-workers (1, 8), with the following modifications. One milliliter of reaction mixture contained 40 mM HEPES-KOH (pH 7.5), 50 mM $(NH_4)_2SO_4$, 4 mM $MgCl_2$, 4 mM creatine phosphate, about 30 U of creatine kinase, 1 mM ATP, 10 μl of [γ-^{32}P]ATP (3000 Ci mmol^{-1}, Amersham), and 3×10^4 U of *E. coli* polyphosphate kinase (PPK) which was purified from PPK-overexpressing *E. coli*, as previously reported (1). After 4 h at 37°C, 100 μl of 0.5 M EDTA (pH 8.0) was added to stop the reaction. Size exclusion chromatography was performed to eliminate unincorporated ATP, using a PD-10 column (Amersham) with elution buffer of 1× TE (pH 8.0) with 100 mM NaCl. Eluted [^{32}P]poly P was precipitated by addition of a 0.75 × volume of isopropanol. After incubating at room temperature for 20 min, [^{32}P]poly P was recovered by centrifugation at 20,000 × *g* for 10 min. The pellet was rinsed with 70% ethanol twice, dried by vacuum centrifugation, and resuspended in 100 μl of distilled water. The chain length of the [^{32}P]poly P was assumed to be close to 750 phosphate residues (8, 15). Unlabeled poly P_{750} was also prepared as described above, but without the addition of [^{32}P]ATP. Short-chain [^{32}P]poly Ps were prepared by limited hydrolysis of [^{32}P]poly P_{750} in 10 mM HCl at 37°C for 30, 60, 90, 120, 180, and 240 min. The various short-chain poly P preps were mixed together in a tube.

The equilibrium binding activity of PPBD to poly P_{750} was measured by rapid filtration assay. PPBD was incubated in 50 μl of reaction mixture (25 mM Tris-HCl [pH 8.3], 137 mM NaCl, 2.7 mM KCl, 2 μg ml^{-1} [69 pmol ml^{-1}] PPBD and the desired concentration of [^{32}P]poly P_{750}) at 0°C for 2 h. The reaction mixture was rapidly applied to a mixed cellulose membrane filter (0.45-μm pore size, 24 mm diameter, Millipore, Billerica, Ma.) pre-wetted with ice-cold washing buffer (25 mM Tris-HCl [pH 8.3], 137 mM NaCl, 2.7 mM KCl) on a vacuum filtration device. The filter was rinsed three times with 1 ml of ice-cold washing buffer and dried at room temperature. The bound polyP was quantified by liquid scintillation counting (LS6500, Beckman, Fullerton, Calif.). When 2000 pmol of

[^{32}P]poly P_{750} was applied to the filter in the absence of PPBD and rinsed with the washing buffer, only 0.2% of the poly P was bound to the filter.

To characterize the reactivity of PPBD to short-chain poly P, the chain length of unbound poly P to the PPBD was analyzed by PAGE. The PPBD was incubated in 10 μl of reaction mixture (25 mM Tris-HCl [pH 8.3], 137 mM NaCl, 2.7 mM KCl, 40 μM of partially hydrolyzed [^{32}P]poly P in terms of Pi and the desired concentration of PPBD) at 0°C for 2 h. The reaction mixture was rapidly applied to the membrane filter, and the filter was rinsed with 1 ml of ice-cold distilled water as described above. Bound poly P on the membrane filter was quantified by liquid scintillation counting. The reaction mixture that passed through the membrane filter was collected in a glass vial and concentrated by vacuum centrifugation. Poly P analysis by PAGE was performed as described by Clark and Wood (19). Two microliters of the sample containing loading dye solution (1× TBE, 10% sucrose and 0.025% bromophenol blue) was loaded on a 15% polyacrylamide gel (370 mm high × 280 mm wide × 0.35 mm thick) with 1× TBE buffer. The electrophoresis was run at 1000 V until the bromophenol blue had migrated 14 cm. The gel was analyzed by a Molecular Imager System (Bio-Rad) with a Storage Phosphor Screen (Kodak, Rochester, N.Y.). Radioactive poly P size markers (poly $P_{39\pm2}$, $P_{56\pm3}$, $P_{88\pm5}$, and $P_{112\pm6}$) and a non-radioactive marker (poly $P_{58\pm10}$) were prepared by extracting poly P bands from the PAGE gel of limitedly hydrolyzed poly P. [γ-^{32}P]ATP, limitedly hydrolyzed [^{32}P]poly P, and completely hydrolyzed [^{32}P] poly P as [^{32}P] orthophosphate were also used as size markers.

Competitive binding assay for PPBD. Inhibition of binding of [^{32}P]poly P_{750} was assayed by unlabeled phosphate compounds: DNA (1 kb Plus DNA Ladder, Invitrogen), RNA (Yeast Total RNA, Ambion, Austin, Tex.), poly P_{750}, poly P type 75+ (Sigma), poly P type 35 (Sigma), poly P type 5 (Sigma), sodium tripolyphosphate (Sigma), sodium pyrophosphate (Sigma) and sodium phosphate (Wako, Osaka, Japan). PPBD was incubated in 50 μl of reaction mixture (25 mM Tris-HCl [pH 8.3], 137 mM NaCl, 2.7 mM KCl, 2 μg ml^{-1} [69 pmol ml^{-1}] PPBD, 40 μM [^{32}P]poly P_{750} in terms of Pi and desired concentration of competitor) at 0°C for 2 h. The reaction mixture was rapidly transferred to the mixed

cellulose membrane filter on a vacuum filtration device. The filter was rinsed three times with 1 ml of ice-cold washing buffer and dried at room temperature. The bound [^{32}P]poly P_{750} was quantified by liquid scintillation counting. By using GraphPad Prism version 4.00 for Windows (GraphPad Software, San Diego, Calif.), the inhibition constant (K_i) was calculated from a model for competitive binding to two sites: $Y = SITE_1+SITE_2+NS$ (31), where Y is the total binding of [^{32}P]poly P_{750}, $SITE_1 = Hot\times B_{max1}/(Hot+K_{d1}\times(1+Cold/K_{i1}))$; $SITE_2 = Hot\times B_{max2}/(Hot+K_{d2}\times(1+Cold/K_{i2}))$, and NS is nonspecific binding; "Hot" is the concentration of [^{32}P]poly P_{750} added to each tube and "Cold" is the concentration of unlabeled phosphate compound (competitor) added, B_{max1} and B_{max2} are the maximum bindings of the [^{32}P]poly P_{750} for each site, K_{d1} and K_{d2} are the dissociation constant (K_d) of the [^{32}P]poly P_{750} for each site, and K_{i1} and K_{i2} are K_i of the [^{32}P]poly P_{750} for each site.

Quantification of poly P in *S. cerevisiae*. Poly P was extracted from 2 ml of the yeast culture as described by Ogawa et al. (32). The Poly P content was measured by *E. coli* PPK assay (8). Poly P was assayed in a 20-μl reaction mixture (40 mM HEPES-KOH [pH 7.5], 40 mM $(NH_4)_2SO_4$, 4 mM $MgCl_2$, 40 μM ADP, 600 U PPK) incubated at 37°C for 40 min and then at 90°C for 2 min. The reaction mixture was diluted 1:100 with 100 mM Tris-HCl [pH 8.0] containing 4 mM EDTA, of which 20 μl was added to the same volume of CLSII reaction mixture (Roche Diagnostics, Basel, Switzerland). Chemiluminescence was measured with a Luminescencer PSN (Atto, Tokyo, Japan) as the total luminescence count in 10 s. The concentration of poly P is given in terms of Pi residues.

PAGE of *S. cerevisiae* poly P. Five milliliters of culture solution was centrifuged and suspended in 400 μl acetone. The cells were disrupted by a bead beater (BioSpec Products, Bartlesville, Okla.) for 10 s three times at 5000 rpm using 200 mg of zirconia beads (0.5 mm in diameter). Acetone was evaporated by vacuum centrifugation. The pellet was suspended in 400 μl distilled water, and the suspension was extracted by phenol:chloroform followed by chloroform extraction. The aqueous phase was used for poly P analysis by PAGE. Two microliters of the sample containing the loading dye solution was loaded on 15% and 8% polyacrylamide gels with 1× TBE buffer. The electrophoresis was run at 1000 V until the bromophenol blue had migrated 14 cm. The gel

was soaked in 10% methanol – 10% acetate for 10 min, stained with 0.5% TBO – 25% methanol – 5% acetate – 5% glycerol for 10 min, and then destained in 25% methanol – 5% acetate – 5% glycerol.

Quick-freezing and freeze-substitution. One milliliter of yeast culture was centrifuged and a portion of the precipitate was transferred onto a formvar membrane spread around a copper loop with a handle (3 mm in diameter; 15 mm long). The loop was further covered by a formvar membrane, and excess water on the loop was removed with a piece of filter paper. The loop was then quickly frozen by plunging it into liquid propane cooled with liquid nitrogen. Frozen samples were transferred to a substitution medium of 100% dry acetone containing Molecular Sieves 4A 1/16 (Wako). The samples were substituted at –80°C for 3 days and warmed at –20°C for 2 h, 4°C for 2 h, and room temperature for 2 h. The samples were immersed twice in 100% dry acetone for 10 min before being infiltrated with Spurr's resin mixed with acetone (25% resin, 50% resin, 75% resin; 12 h for each step) and then with pure resin for 2 days (resin was replaced once at 24 h). The samples were polymerized at 70°C overnight. Embedded materials were sectioned with an ultramicrotome (Leica, Bannockburn, Ill.). Sections about 70 nm thick for electron microscopy were cut with a diamond knife and picked up on 200-mesh nickel grids. Semithin sections were cut with glass knives to 300-nm thickness and collected on aminosilane-coated glass slides (Matsunami, Osaka, Japan).

Poly P detection using PPBD affinity labeling under laser scanning confocal microscopy (LSCM). Sections were immersed for 10 min at room temperature in methanol containing 10% H_2O_2 . The sections were washed with distilled water. Specimens were blocked for 10 min at room temperature with Tris-buffered saline (pH 8.3) (TBS) containing 1% BSA. Samples were first incubated at room temperature overnight in a mixture of 20 μg ml^{-1} PPBD, 10 μg ml^{-1} mouse anti-Xpress epitope antibody (Invitrogen), TBS, and 1% BSA. Samples were washed with TBS containing 0.05% Triton X-100 with or without 0.2 M imidazole, then washed with TBS. Semithin sections were incubated for 2 h at room temperature with a goat anti-mouse IgG antibody conjugated with Alexa 488 (Molecular Probes, Eugene, Ore.) diluted 1:5000 in TBS containing 1% BSA. Samples

were sequentially washed with TBS containing 0.05% Triton X-100, TBS, and distilled water. Negative controls were prepared by incubating sections without PPBD, mouse anti-Xpress antibody or labeled goat anti-mouse IgG antibody; or without both PPBD and mouse anti-Xpress antibody. Another negative control was prepared by incubating sections with an excessive amount of competitor (100 mM tripolyphosphate) during the first reaction. Fluorescence microscopy was performed by LSCM (LSM510, Carl Zeiss, Jena, Germany). The fluorescence of Alexa 488 was excited by using a 488-nm-wavelength argon laser, and the fluorescence emitted was detected with a 505–550-nm band-pass filter. Autofluorescence was detected with a 580–nm long-pass filter using a 546-nm He–Ne laser for excitation. Image analysis was performed with LSM 510 Software version 2.5 (Carl Zeiss).

Poly P detection using PPBD affinity labeling under transmission electron microscopy (TEM). Ultrathin sections were immersed in the H_2O_2–methanol, blocked in TBS containing BSA, and incubated in a mixture of PPBD, mouse anti-Xpress epitope antibody, TBS, and BSA, as described above for LSCM. The ultrathin sections were incubated for 2 h at room temperature with a goat anti-mouse IgG antibody conjugated with 10 nm colloidal gold (BBInternational, Cardiff, UK), diluted 1:100 in TBS containing 1% BSA. After labeling, the ultrathin sections were stained with uranyl acetate followed by lead citrate and observed by TEM (H-7100, Hitachi, ,Tokyo, Japan) at an accelerating voltage of 75 kV.

Results

Purification of PPBD. To obtain PPBD for poly P labeling, we constructed an expression vector in which the PPBD sequence was linked to sequences of the Xpress epitope and 6×His. The Xpress epitope was used to detect PPBD localization by immunocytochemistry, and the 6×His was used for purification by affinity chromatography. The PPBD expressed in *E. coli* was purified using a Ni^{2+}-charged affinity column. To elute PPBD from the affinity column, approximately 0.2 M imidazole was required. The eluted PPBD was purified as a single band by SDS-PAGE analysis, and its size was approximately 29 kDa (Fig. 1A).

Binding assay of PPBD. Equilibrium binding of poly P_{750} to PPBD is shown in Figure 2A. Scatchard transform of the equilibrium binding yielded two binding sites (Fig. 2B): a high-affinity site (K_{d1} = 2.0 μM as Pi) and a lower affinity site (K_{d2} = 12.0 μM as Pi).

An equilibrium binding experiment of mildly hydrolyzed poly P to PPBD was carried out to characterize the PPBD affinity for short-chain poly P. From PAGE analysis of unbound poly P, the distribution of the unbound poly P chain length was shown to shift to short chain as the PPBD concentration increased (Fig. 3A). When 40 μM of mildly hydrolyzed poly P was incubated with 3.4×10^4 pmol ml^{-1} PPBD in which poly P binding sites were almost saturated (Fig. 3B), PPBD bound to most poly P longer than 35 residues. PPBD at concentrations of 6.9×10^3 and 1.4×10^3 pmol ml^{-1} bound to > poly P_{50} and > poly P_{80}, respectively. PPBD bound to only a small amount of short poly P (< 30 residues), even when a high concentration of PPBD was used.

To determine the affinity of PPBD for short-chain poly P and other high molecular weight phosphate compounds, we compared the inhibition of poly P_{750} binding among the phosphate compounds. Some poly P reagents obtained from Sigma are known to be mixtures of a wide range of poly Ps (19, 55). Poly P type 75+ consisted mainly of poly P longer than 40 residues (Fig. 4C). Poly P type 35 and type 5 consisted of polyP shorter than 120–150 and 20 residues, respectively (Fig. 4C). The curves in Figure 4 and K_i values in Table 1 were calculated by nonlinear regression using a model for competitive binding to two sites. As the poly P chain length of competitors became shorter, the K_i value of

[^{32}P]poly P_{750} binding increased (Fig. 4A and Table 1). Orthophosphate hardly inhibited [^{32}P]poly P_{750} binding to PPBD. The affinities of PPBD for poly P type 75+, poly P type 35, poly P type 5, tripolyphosphate, pyrophosphate, and orthophosphate were about 7–8, 35, 260, 80, 230, and 3200 times lower, respectively, than that for poly P_{750}. The K_i value by DNA was almost equal to that by poly P type 35 when the concentration of nucleic acid was expressed by molar values in terms of Pi (Fig. 4B and Table 1). The K_i value by RNA was between that by poly P type 35 and tripolyphosphate. When the nucleic acid concentration was expressed in milligrams per milliliter, the K_i value by DNA was between that for tripolyphosphate and pyrophosphate, and the K_i value by RNA was nearly equal to that by pyrophosphate (data not shown).

Poly P content and length in *S. cerevisiae*. The poly P content of *S. cerevisiae* incubated in YPD-high Pi for 10 h was 2383 nmol as Pi mg^{-1} protein, which was 340 times higher than the poly P content (7 nmol as Pi mg^{-1} protein) of *S. cerevisiae* incubated in YPD-low Pi. The chain length of poly P extracted from *S. cerevisiae* in YPD-high Pi was less than 150 residues in PAGE analysis (Fig. 5). Longer chains of poly P were detected in 8% PAGE analysis (Fig. 5, lane 4), but their amounts were very low.

Poly P labeling using PPBD affinity (LSCM). Poly P localization was visualized by fluorescence-based poly P labeling using PPBD affinity (Fig. 6). Initially, sections were sequentially incubated in PPBD solution, anti-Xpress antibody solution, and anti-mouse IgG antibody solution. This procedure gave a highly fluorescent background. This problem was overcome by sequentially incubating the sections in a solution of PPBD – anti Xpress antibody complex and then anti-mouse IgG antibody solution. Signals from labeled poly P were exhibited as green fluorescence of Alexa 488, but some green fluorescence was derived from autofluorescence of collapsed cells. The poly P signal could be discriminated from autofluorescence by overlaying images excited by He–Ne laser (wavelength 546 nm), because the autofluorescence had a broad emission spectrum. Intense labeling was observed in the vacuoles (Fig. 6a, b). The distribution in vacuoles was dispersed (Fig. 6b). Many cells incubated in YPD-high Pi contained poly P, but not all cells (Fig. 6a). In YPD-low Pi, few cells showed the poly P signal (Fig. 6c). No poly P signal was detected in the negative

controls, from which PPBD and/or antibody had been removed from the reaction mixture (Fig. 6d, e, f, g), or in which the poly P binding site of PPBD had been saturated with a high concentration of tripolyphosphate (Fig. 6h).

Poly P labeling using PPBD affinity (TEM). An ultrastructural method of poly P detection was developed using TEM. With this method, colloidal gold instead of the fluorescent probe was conjugated to the secondary antibody. When the samples were fixed, osmium tetroxide was not used because the reagent reduced the poly P signal intensity (data not shown). Most signals were observed in the vacuoles of *S. cerevisiae* in YPD-high Pi (Fig. 7a, b, c, d). The density of colloidal gold in vacuoles was different among cells, even in the same section: dense (Fig. 7a) to sparse (Fig. 7b) to no signal (data not shown). Poly P signals were found all over the vacuole and seemed to be located on flocculent material within the vacuole. The poly P distribution was not completely homogenous within individual vacuoles: some regions were dense, and some were sparse (Fig. 7c). In most cells signals were barely observed in the nuclei and mitochondria (Fig. 7a, c), although some signals were often observed around the vacuoles (Fig. 7c, d). However, we did not determine whether the poly P signals were in or on a certain organelle or in the cytoplasm. This is because osmium tetroxide was not used for fixation, and there was low contrast for membrane structure. Intense signals were not observed in the cells incubated in YPD-low Pi, whereas a few signals were occasionally found around the vacuoles (data not shown). There was no poly P signal in the negative controls, where sections of *S. cerevisiae* (YPD-high Pi) were incubated in reaction mixture without PPBD (Fig. 7e), without mouse anti-Xpress antibody (Fig. 7e), without both PPBD and mouse anti-Xpress antibody (data not shown), or without goat anti-mouse IgG antibody conjugated with 10 nm colloidal gold (data not shown). There was also no poly P signal when the poly P binding site of PPBD was masked with a high concentration of tripolyphosphate. To check for non-specific binding of PPBD by 6×His tag, sections were washed with an imidazole-containing buffer after PPBD incubation. The signal distribution was not different between treatments with and without imidazole, indicating that 6×His tag did not affect the poly P labeling.

Discussion

We developed a novel procedure to specifically detect poly P with high spatial resolution at the ultrastructural level. EDXS and EELS detect phosphorus elements, but no direct detection method for poly P at the ultrastructural level has been available. A novel point of the procedure was to use PPBD linked with an epitope tag. Immunocytochemical methods are usually used to investigate the localization of biological molecules. However, it seemed difficult to use immunological techniques in the analysis of poly P localization because of the difficulty in raising specific antibodies against poly P. We examined the use of PPX, which exhibits specific binding to poly P in the evolutional process. One of the methods that uses the specific affinity of an enzyme to its substrate is the enzyme–gold procedure, where an enzyme directly bound colloidal gold is applied to sections and then the substrate is visualized as signals of colloidal gold (11). Initially, we tried the enzyme–gold procedure in which purified PPX bound to the colloidal gold was used. The PPX–gold complex exhibited little binding activity to poly P (data not shown). This may have been because the poly P binding site of the PPX was masked by the colloidal gold. Next, we developed a method in which an epitope tag on PPBD bound to poly P was detected immunocytochemically.

Affinity assays of PPBD and control experiments of poly P labeling showed that fluorescent and colloidal gold signals by the poly P labeling specifically represented poly P localization. Cellular poly P consists of polymers of various chain length. PPX has been reported to have poly P binding sites on its C-terminal domain (15), but their affinities to various lengths of poly P or other phosphate compounds, including nucleic acids, were unknown. The competitive binding assay (Fig. 4B and Table 1) indicated that the PPBD of PPX binds strongly to long-chain poly P but is not able to bind short-chain poly P unless the poly P exists in high concentration. Unexpectedly, poly P type 5 showed lower affinity than did tripolyphosphate and pyrophosphate (Table 1). This could be because the poly P type 5 contains orthophosphate, pyrophosphate, and tripolyphosphate other than poly P_4–P_{20}. From the binding assay, we found that poly P labeling using PPBD was suitable for detecting long-chain poly P. However, it may be difficult to detect short-chain poly P

because of the low affinity. It is also possible that short-chain poly P was eluted from the sections during labeling. The affinity of the PPBD for nucleic acid was not as high as that for long-chain poly P. The low affinity to nucleic acid was also confirmed from poly P labeling of yeast, in which few colloidal gold particles were observed on DNA in the nuclei and mitochondria. In a preliminary experiment of poly P labeling using PPBD, the addition of osmium tetroxide to samples for ultrastructural analysis led to a reduction in the poly P signal. This would be because the osmium forms complexes with poly P and then the amount of free poly P available to bind to the PPBD decreases. Another point of note is that poly P signals gradually decrease with time after the sections are made. This may be because poly P in sections is degraded or oxidized, so that the PPBD cannot then bind to these compounds.

The size of yeast poly P was less than about 150 residues when the yeast was incubated in Pi-rich medium (Fig. 5). This size distribution is similar to that of poly P type 35. Therefore the affinity of PPBD for the yeast poly P would be similar to that for the poly P 35 in the phosphate compounds tested. Most poly P was distributed in vacuoles (Figs. 6 and 7). This result was consistent with a study of subcellular fractionation (53), in which the vacuole fraction was shown to contain large amounts of poly P. However, Trilisenko et al. (51) reported that vacuolar poly P of yeast accounted for only about 15% of the total poly P, and suggested that the vacuolar poly P content is dependent on the strain, culture conditions, developmental stage, or method of vacuole isolation. Orlovich and Ashford (33) demonstrated that phosphorus observed by EDXS was evenly dispersed in vacuoles when *Pisolithus tinctorius* hyphae were fixed by cryofixation and freeze-substitution, although the fungal vacuoles were treated by conventional chemical fixation and contained precipitated phosphorus-rich granules. They suggested that the precipitated granules were artifacts caused by dehydration during chemical fixation and that vacuolar poly P exists in a soluble form in living cells. On the other hand, Bücking and Heyser (17) observed granules in the vacuoles of living hyphae with light microscopy and showed by EDXS analysis of cryofixed and freeze-dried samples that there were phosphorus-containing granules in the vacuoles. In our observation of yeast cells, vacuolar poly P was dispersed, not precipitated,

when the cells were fixed by quick-freezing and freeze-substitution. More detailed observation revealed that the poly P distribution in the vacuoles was somewhat heterogeneous (Fig. 7c). Under our experimental conditions, we did not observe electron-dense structures, such as poly P granules, in the vacuoles or cytoplasm. Then, we could not examine whether the poly P detection method is available for the granule form. Poly P granules have been isolated from yeast cells under poly P overcompensation conditions in which phosphate-starved yeast cells are incubated in phosphate-rich medium (21). Therefore, there is a possibility that poly P in yeast cells could be taken as two forms, soluble or precipitated, depending on the cultural conditions, on physiological state of the cells, and/or on a process of poly P accumulation. Further researches on the form and localization of poly P in yeast cells are necessary in terms of cultural conditions and physiological states.

Poly P was also observed at low density around the vacuoles (Fig. 7c, d). It was not clear whether the poly P was in the cytosol, endoplasmic reticulum, or other organelles, because osmium tetroxide was omitted during the fixation, thus reducing the image contrast. However, strong evidence for the presence of poly P in non-vacuolar compartments has been provided by subcellular fractionation and cytological staining. Trilisenko et al. (51) showed that the cytosol fraction of yeast contained much poly P. Other circumstantial evidence of cytosolic poly P is the fact that yeast exopolyphosphatase (PPX1) has been isolated from the cytosol fraction (56, 57), implying that poly P, a substrate of PPX1, exists in the cytosol. In our study, poly P signals were barely detectable in the nuclei and mitochondria. However, several studies have showed that poly P is detected in the nuclei of *Neurospora crassa*, *Endomyces magnusii* (26) and mammalian cells (27) by using cell fractionation, and in yeast mitochondria by ^{31}P NMR (10). The amounts of poly P in the nuclei and mitochondria are not very high compared with the vacuolar poly P. Poly P in yeast mitochondria consists of short chains less than 15 residues (34). Because of the small amount of poly P present or its short chain length, our procedure using PPBD might not have detected poly P signals in the mitochondria. Many researchers have described poly P in the cell periphery, the cell envelope or cell wall in yeasts (48–50,

54) and *E. magnusii* (26). However, we could not detect poly P signals in such structures in *S. cerevisiae*. The presence of poly P in the structures seems to depend on the fungal species and incubation conditions. Tijssen et al. (48) showed that poly P on the cell envelope was detected in *Saccharomyces fragilis* by DAPI staining but not in *S. cerevisiae*. However, *S. cerevisiae* can accumulate poly P on the outer membrane when the cells are incubated in Pi-rich medium after phosphate starvation (54).

In summary, we demonstrated a new technique, based on enzymatic affinity and immunocytochemistry, for the analysis of poly P localization. We also showed that most of the long-chain poly P detected by our procedure was distributed in the yeast vacuoles in a dispersed manner, and a much smaller amount of poly P was localized around the vacuoles. This poly P detection method will provide new insight into the biology of poly P. Furthermore, we expect that this kind of method will be applicable to the detection of other biological macromolecules.

Acknowledgments

We thank Dr. Arthur Kornberg and his co-workers for their kind distribution of the PPK over-expressing *E. coli* strain. We thank Dr. R. Larry Peterson for his valuable suggestions and critical reading of the manuscript. This work was supported in part by the Promotion of Basic Research Activities for Innovative Biosciences (PROBRAIN) of the Bio-oriented Technology Research Advancement Institution, Japan. KS was awarded an Organization for Economic Co-operation and Development (OECD) Fellowship under the Co-operative Research Programme: Biological Resource Management for Sustainable Agricultural Systems.

References

1. **Ahn, K., and A. Kornberg.** 1990. Polyphosphate kinase from *Escherichia coli*. purification and demonstration of a phosphoenzyme intermediate. J. Biol. Chem. **265:**11734–11739.
2. **Allan, R. A., and J. J. Miller.** 1980. Influence of *S*-adenosylmethionine on DAPI-induced fluorescence of polyphosphate in the yeast vacuole. Can. J. Microbiol. **26:**912–920.
3. **Ashford, A. E.** 1998. Dynamic pleiomorphic vacuole systems: are they endosomes and transport compartments in fungal hyphae? p. 119–159. *In* J. A. Callow (ed.), Adv. Bot. Res., vol. 28. Academic Press, San Diego.
4. **Ashford, A. E., L. Cole, and G. J. Hyde.** 2001. Motile tubular vacuole systems, p. 243–265. *In* R. J. Howard and N. A. R. Gow (ed.), The Mycota: biology of the fungal cell, vol. VIII. Springer-Verlag, Berlin.
5. **Ashford, A. E., M. Ling-Lee, and G. A. Chilvers.** 1975. Polyphosphate in eucalypt mycorrhizas: a cytochemical demonstration. New Phytol. **74:**447–453.
6. **Ashford, A. E., R. L. Peterson, D. Dwarte, and G. A. Chilvers.** 1986. Polyphosphate granules in eucalypt mycorrhizas: determination by energy dispersive X-ray microanalysis. Can. J. Bot. **64:**677–687.
7. **Ashford, A. E., P. A. Vesk, D. A. Orlovich, A-L. Markovina, and W. G. Allaway.** 1999. Dispersed polyphosphate in fungal vacuoles in *Eucalyptus pilularis*/*Pisolithus tinctorius* ectomycorrhizas. Fungal Genet. Biol. **28:**21–33.
8. **Ault-Riché, D., C. D. Fraley, C-M. Tzeng, and A. Kornberg.** 1998. Novel assay reveals multiple pathways regulating stress-induced accumulations of inorganic polyphosphate in *Escherichia coli*. J. Bacteriol. **180:**1841–1847.
9. **Baxter, M., and T. E. Jensen.** 1986. Cell volume occupied by polyphosphate bodies during the polyphosphate overplus phenomenon in *Plectonema boryanum*. Cytobios **45:**147–160.
10. **Beauvoit, B., M. Rigoulet, B. Guerin, and P. Canioni.** 1989. Polyphosphates as a source of high energy phosphates in yeast mitochondria: a ^{31}P NMR study. FEBS

Lett. **252:**17–21.

11. **Bendayan, M.** 1989. The enzyme-gold cytochemical approach: a review, p. 117–147, Colloidal gold: principles, methods, and applications, vol. 2. Academic Press, San Diego.
12. **Boddington, C. L., and J. C. Dodd.** 1999. Evidence that differences in phosphate metabolism in mycorrhizas formed by species of *Glomus* and *Gigaspora* might be related to their life-cycle strategies. New Phytol. **142:**531–538.
13. **Bode, G., F. Mauch, H. Ditschuneit, and P. Malfertheiner.** 1993. Identification of structures containing polyphosphate in *Helicobacter pylori*. J. Gen. Microbiol. **139:**3029–3033.
14. **Bolesch, D. G., and J. D. Keasling.** 2000. The effect of monovalent ions on polyphosphate binding to *Escherichia coli* exopolyphosphatase. Biochem. Biophys. Res. Comm. **274:**236–241.
15. **Bolesch, D. G., and J. D. Keasling.** 2000. Polyphosphate binding and chain length recognition of *Escherichia coli* exopolyphosphatase. J. Biol. Chem. **275:**33814–33819.
16. **Bücking, H., S. Beckmann, W. Heyser, and I. Kottke.** 1998. Elemental contents in vacuolar granules of ectomycorrhizal fungi measured by EELS and EDXS. a comparison of different methods and preparation techniques. Micron **29:**53–61.
17. **Bücking, H., and W. Heyser.** 1999. Elemental composition and function of polyphosphates in ectomycorrhizal fungi – an X-ray microanalytical study. Mycol. Res. **103:**31–39.
18. **Castuma, C. E., R. Huang, A. Kornberg, and R. N. Reusch.** 1995. Inorganic polyphosphates in the acquisition of competence in *Escherichia coli*. J. Biol. Chem. **270:**12980–12983.
19. **Clark, J. E., and H. G. Wood.** 1987. Preparation of standards and determination of sizes of long-chain polyphosphates by gel electrophoresis. Anal. Biochem. **161:**280–290.
20. **Cole, L., D. A. Orlovich, and A. E. Ashford.** 1998. Structure, function, and

motility of vacuoles in filamentous fungi. Fungal Genet. Biol. **24:**86–100.

21. **Jacobson, L., M. Halmann, and J. Yariv.** 1982. The molecular composition of the volutin granule of yeast. Biochem. J. **201:**473–479.

22. **Jäger, K. M., C. Johansson, U. Kunz, and H. Lehmann.** 1997. Sub-cellular element analysis of a cyanobacterium (*Nostoc* sp.) in symbiosis with *Gunnera manicata* by ESI and EELS. Bot. Acta **110:**151–157

23. **Kaffman, A., I. Herskowitz, R. Tjian, and E. K. O'Shea.** 1994. Phosphorylation of the transcription factor PHO4 by a cyclin-CDK complex, PHO80-PHO85. Science **263:**1153–1156.

24. **Kim, K-S., N. N. Rao, C. D. Fraley, and A. Kornberg.** 2002. Inorganic polyphosphate is essential for long-term survival and virulence factors in *Shigella* and *Salmonella* spp. Proc. Nat. Acad. Sci. **99:**7675–7680.

25. **Kornberg, A., N. N. Rao, and D. Ault-Riché.** 1999. Inorganic polyphosphate: a molecule of many functions. Annu. Rev. Biochem. **68:**89–125.

26. **Kulaev, I. S., V. M. Vagabov, and T. V. Kulakovskaya.** 2004. Localization of polyphosphates in cells of prokaryotes and eukaryotes, p. 53–63. *In* I. S. Kulaev, V. M. Vagabov, and T. V. Kulakovskaya (ed.), The biochemistry of inorganic polyphosphates, 2nd ed. John Wiley & Sons, West Sussex.

27. **Kumble, K. D., and A. Kornberg.** 1995. Inorganic polyphosphate in mammalian cells and tissues. J. Biol. Chem. **270:**5818–5822.

28. **Kuroda, A., K. Nomura, R. Ohtomo, J. Kato, T. Ikeda, N. Takiguchi, H. Ohtake, and A. Kornberg.** 2001. Role of inorganic polyphosphate in promoting ribosomal protein degradation by the Lon protease in *E. coli*. Science **293:**705–708.

29. **Kuroda, A., S. Tanaka, T. Ikeda, J. Kato, N. Takiguchi, and H. Ohtake.** 1999. Inorganic polyphosphate kinase is required to stimulate protein degradation and for adaptation to amino acid starvation in *Escherichia coli*. Proc. Nat. Acad. Sci. **96:**14264–14269.

30. **Marchesini, N., F. A. Ruiz, M. Vieira, and R. Docampo.** 2002. Acidocalcisomes are functionally linked to the contractile vacuole of *Dictyostelium discoideum*. J.

Biol. Chem. **277:**8146–8153.

31. **Motulsky, H., and A. Christopoulos.** 2003. Fitting models to biological data using linear and nonlinear regression. A practical guide to curve fitting. GraphPad Software, San Diego.
32. **Ogawa, N., J. DeRisi, and P. O. Brown.** 2000. New components of a system for phosphate accumulation and polyphosphate metabolism in *Saccharomyces cerevisiae* revealed by genomic expression analysis. Mol. Biol. Cell **11:**4309–4321.
33. **Orlovich, D. A., and A. E. Ashford.** 1993. Polyphosphate granules are an artefact of specimen preparation in the ectomycorrhizal fungus *Pisolithus tinctorius*. Protoplasma **173:**91–102.
34. **Pestov, N. A., T. V. Kulakovskaya, and I. S. Kulaev.** 2004. Inorganic polyphosphate in mitochondria of *Saccharomyces cerevisiae* at phosphate limitation and phosphate excess. FEMS Yeast Res. **4:**643–648.
35. **Rao, N. N., S. Liu, and A. Kornberg.** 1998. Inorganic polyphosphate in *Escherichia coli*: the phosphate regulon and the stringent response. J. Bacteriol. **180:**2186–2193.
36. **Rashid, M. H., and A. Kornberg.** 2000. Inorganic polyphosphate is needed for swimming, swarming, and twitching motilities of *Pseudomonas aeruginosa*. Proc. Nat. Acad. Sci. **97:**4885–4890.
37. **Rashid, M. H., N. N. Rao, and A. Kornberg.** 2000. Inorganic polyphosphate is required for motility of bacterial pathogens. J. Bacteriol. **182:**225–227.
38. **Rees, G. N., G. Vasiliadis, J. W. May, and R. C. Bayly.** 1992. Differentiation of polyphosphate and poly-beta-hydroxybutyrate granules in an *Acinetobacter* sp. isolated from activated sludge. FEMS Microbiol. Lett. **73:**171–173.
39. **Rodrigues, C. O., F. A. Ruiz, P. Rohloff, D. A. Scott, and S. N. J. Moreno.** 2002. Characterization of isolated acidocalcisomes from *Toxoplasma gondii* tachyzoites reveals a novel pool of hydrolyzable polyphosphate. J. Biol. Chem. **277:**48650–48656.
40. **Rubin, G. M.** 1973. The nucleotide sequence of *Saccharomyces cerevisiae* 5.8 S

ribosomal ribonucleic acid. J. Biol. Chem. **248:**3860–3875.

41. **Ruiz, F. A., N. Marchesini, M. Seufferheld, Govindjee, and R. Docampo.** 2001. The polyphosphate bodies of *Chlamydomonas reinhardtii* possess a proton-pumping pyrophosphatase and are similar to acidocalcisomes. J. Biol. Chem. **276:**46196–46203.

42. **Ruiz, F. A., C. O. Rodrigues, and R. Docampo.** 2001. Rapid changes in polyphosphate content within acidocalcisomes in response to cell growth, differentiation, and environmental stress in *Trypanosoma cruzi*. J. Biol. Chem. **276:**26114–26121.

43. **Schröder, H. C., B. Lorenz, L. Kurz, and W. E. G. Müller.** 1999. Inorganic polyphosphate in eukaryotes: enzymes, metabolism and function, p. 45–81. *In* H. C. Schröder and W. E. G. Müller (ed.), Prog. Mol. Subcell. Biol., vol. 23. Springer-Verlag, Berlin.

44. **Serafim, L. S., P. C. Lemos, C. Levantesi, V. Tandoi, H. Santos, and M. A. M. Reis.** 2002. Methods for detection and visualization of intracellular polymers stored by polyphosphate-accumulating microorganisms. J. Microbiol. Methods **51:**1–18.

45. **Shiba, T., D. Nishimura, Y. Kawazoe, Y. Onodera, K. Tsutsumi, R. Nakamura, and M. Ohshiro.** 2003. Modulation of mitogenic activity of fibroblast growth factors by inorganic polyphosphate. J. Biol. Chem. **278:**26788–26792.

46. **Shiba, T., K. Tsutsumi, H. Yano, Y. Ihara, A. Kameda, K. Tanaka, H. Takahashi, M. Munekata, N. N. Rao, and A. Kornberg.** 1997. Inorganic polyphosphate and the induction of *rpoS* expression. Proc. Nat. Acad. Sci. **94:**11210–11215.

47. **Suresh, N., R. Warburg, M. Timmerman, J. Wells, M. Coccia, M. F. Roberts, and H. O. Halvorson.** 1985. New strategies for the isolation of microorganisms responsible for phosphate accumulation. Water Sci. Technol. **17:**99–111.

48. **Tijssen, J. P. F., H. W. Beekes, and J. van Steveninck.** 1982. Localization of polyphosphates in *Saccharomyces fragilis*, as revealed by 4′,6-diamidino-2-phenylindole fluorescence. Biochem. Biophys. Acta **721:**394–398.

49. **Tijssen, J. P. F., T. M. A. R. Dubbelman, and J. van Steveninck.** 1983. Isolation

and characterization of polyphosphates from the yeast cell surface. Biochem. Biophys. Acta **760:**143–148.

50. **Tijssen, J. P. F., and J. van Steveninck.** 1984. Detection of a yeast polyphosphate fraction localized outside the plasma membrane by the method of phosphorus-31 nuclear magnetic resonance. Biochem. Biophys. Res. Comm. **119:**447–451.
51. **Trilisenko, L. V., V. M. Vagobov, and I. S. Kulaev.** 2002. The content and chain length of polyphosphates from vacuoles of *Saccharomyces cerevisiae* VKM Y-1173. Biochemistry (Moscow) **67:**711–716.
52. **Turnau, K., I. Kottke, and F. Oberwinkler.** 1993. *Paxillus involutus – Pinus sylvestris* mycorrhizae from heavily polluted forest. I. Elemental localization using electron energy loss spectroscopy and imaging. Bot. Acta **106:**213–219.
53. **Urech, K., M. Dürr, T. Boller, and A. Wiemken.** 1978. Localization of polyphosphate in vacuoles of *Saccharomyces cerevisiae*. Arch. Microbiol. **116:**275–278.
54. **Vořišek, J., A. Knotková, and A. Kotyk.** 1982. Fine cytochemical localization of polyphosphates in the yeast *Saccharomyces cerevisiae*. Zbl. Mikrobiol. **137:**421–432.
55. **Wood, H. G., and J. E. Clark.** 1988. Biological aspects of inorganic polyphosphates. Annu. Rev. Biochem. **57:**235–260.
56. **Wurst, H., and A. Kornberg.** 1994. A soluble exopolyphosphatase of *Saccharomyces cerevisiae*. purification and characterization. J. Biol. Chem. **269:**10996–11001.
57. **Wurst, H., T. Shiba, and A. Kornberg.** 1995. The gene for a major exopolyphosphatase of *Saccharomyces cerevisiae*. J. Bacteriol. **177:**898–906.

Figure legends

FIG. 1. (A) SDS-PAGE analysis of purified polyphosphate binding domain (PPBD). Standards and samples were fractionated by 10% SDS-PAGE. Lane 1, size standards (numbers on the left in kDa) and lane 2, purified PPBD. (B) Schematic illustration of poly

P labeling for transmission electron microscopic observation. Poly P in ultrathin sections is treated with PPBD linked by Xpress epitope tag. The epitope tag was detected by indirect immuno-gold labeling using anti-Xpress epitope antibody and secondary antibody conjugated with colloidal gold. For laser scanning confocal microscopic observation, the secondary antibody was conjugated with Alexa 488 instead of colloidal gold.

FIG. 2. Equilibrium binding of poly P_{750} to purified PPBD (A), and Scatchard plot (B). Scatchard transform of equilibrium binding yielded two binding sites.

FIG. 3. Equilibrium binding of limitedly hydrolyzed poly P to PPBD. (A) PAGE (15%) analysis of unbound poly P to PPBD. Lane 1, limitedly hydrolyzed poly P as size ladders; lane 2, ATP; lane 3, orthophosphate; lanes 4–8, poly P unbound to 0, 2.8×10^2, 1.4×10^3, 6.9×10^3, and 3.4×10^4 pmol ml^{-1} PPBD, respectively, and lane 9, poly P size markers. Numbers on both sides indicate chain lengths of poly P. Bands between P_1 and P_2 are hexametaphosphate. (B) Equilibrium binding of limitedly hydrolyzed poly P to PPBD.

FIG. 4. Inhibition of [^{32}P]poly P_{750} binding to PPBD by unlabeled phosphate compounds. (A) Inhibition by various types of poly P. P_{750}, unlabeled poly P_{750}; P_{75}, poly P type 75+; P_{35}, poly P type 35; P_5, poly P type 5; P_3, tripolyphosphate; P_2, pyrophosphate; and P_1, orthophosphate. (B) Inhibition by DNA and RNA. Concentrations are expressed in terms of Pi. (C) Size distribution of poly P type 75+ (lane 1), type 35 (lane 2) and type 5 (lane 3), analyzed by PAGE (15%). Poly P was stained with toluidine blue O. Numbers on the left indicate chain lengths of poly P, which was determined from size ladders of limitedly hydrolyzed [^{32}P]poly P. Value in parenthesis was estimated from Clark and Wood (19).

FIG. 5. PAGE analysis of *Saccharomyces cerevisiae* poly P. Poly P extracted from *S. cerevisiae* cultured in YPD containing 10 mM phosphate (YPD-high Pi) (lanes 2 and 4) was fractionated by 15% (lanes 1 and 2) and 8% (lanes 3 and 4) PAGE. Poly P size markers (lanes 1 and 3) are poly $P_{58\pm10}$. Numbers on the left indicate chain lengths of poly P, which

were determined from size markers. Chain length indicated on the right was estimated from Clark and Wood (19). Some RNA bands were recognized near the top in lane 2 and near residues 150 and 200 of poly P in lane 4.

FIG. 6. Laser scanning confocal images of poly P distribution. Poly P was labeled with PPBD – anti Xpress antibody complex followed by anti mouse IgG antibody conjugated with Alexa 488 (a–c), or various controls (d–f). Fluorescent images of Alexa 488 and autofluorescent images were superimposed with pseudo differential interference contrast images. Fluorescence of Alexa 488 appears green. Some green fluorescence was derived from autofluorescence of collapsed cells. The poly P signal was discriminated from the autofluorescence (yellow to red) by overlaying images excited by He–Ne laser (wavelength 546 nm), because the autofluorescence had a broad emission spectrum. (a) Sections of *Saccharomyces cerevisiae* incubated in YPD containing 10 mM phosphate (YPD-high Pi). Intense poly P signals were detected in vacuoles of *S. cerevisiae* cells. (b) Highly magnified image of *S. cerevisiae* incubated in YPD-high Pi. Poly P is distributed in a dispersed manner in the vacuoles. (c) Sections of *S. cerevisiae* incubated in YPD containing 0.2 mM phosphate (YPD-low Pi). Few poly P signals were detected in the cells. (d–h) Negative controls of poly P labeling using PPBD affinity. Sections of *S. cerevisiae* (YPD-high Pi) were incubated in reaction mixture without PPBD (d), without mouse anti-Xpress antibody (e), without both PPBD and mouse anti-Xpress antibody (f), without goat anti-mouse IgG antibody conjugated with Alexa 488 (g), or in a mixture of PPBD-anti Xpress antibody complex to which had been added 100 mM tripolyphosphate (h). Bar, 5.0 μm.

FIG. 7. Transmission electron micrographs of poly P distribution. Poly P was labeled with PPBD – anti Xpress antibody complex followed by anti mouse IgG antibody conjugated with 10 nm colloidal gold. Sections of *Saccharomyces cerevisiae* were incubated in YPD-high Pi. (a) Poly P signal distribution in a *S. cerevisiae* cell. Intense poly P signals were found in the vacuoles. In the nucleus, few signals were detected. (b) Poly P signals were found in the vacuole, but the signal density was not very high in this cell. (c) Highly

magnified image of a yeast vacuole. Signals were found all over the vacuole, but their distribution was not completely homogenous. Some poly P signals (arrows) were detected around the vacuole. (d) Poly P signals (arrows) around the vacuole. (e, f) Negative controls of poly P labeling using PPBD affinity. Sections of *S. cerevisiae* were incubated in the reaction mixture without PPBD (e), and without mouse anti-Xpress antibody (f). E, endoplasmic reticulum; M, mitochondria; N, nucleus; and V, vacuole. Bar, 500 nm.

TABLE 1. Affinity values of PPBD for phosphate compounds. Inhibition constants (K_i) were determined from displacement of [^{32}P]poly P_{750} binding to poly P binding sites on PPBD.

Competitor	K_{i1} (μM as Pi)	K_{i2}
Poly P_{750}	2	10
Poly P type 75+	13	83
Poly P type 35	70	339
Poly P type 5	533	2,588
Tripolyphosphate	167	807
Pyrophosphate	471	2,280
Orthophosphate	6,592	31,915
DNA	67	324
RNA	131	635

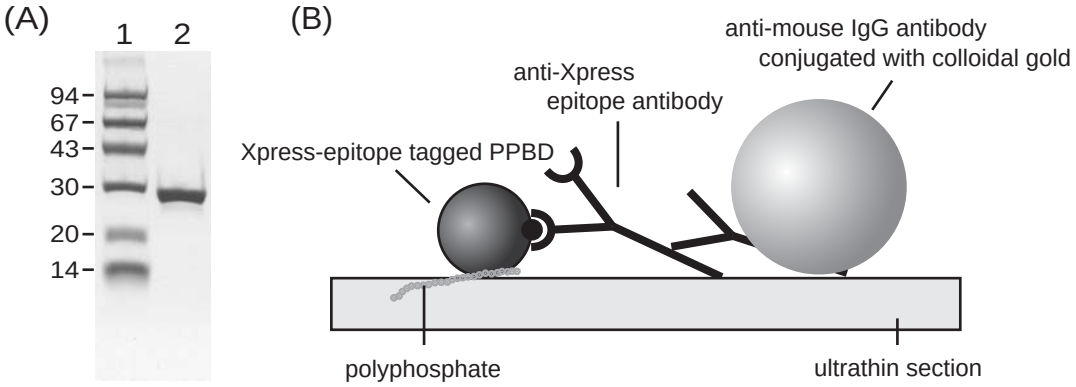
(A)
1
2
94
67
43
30
20
14
(B)
anti-mouse IgG antibody
conjugated with colloidal gold
anti-Xpress
epitope antibody
Xpress-epitope tagged PPBD
polyphosphate
ultrathin section

FIG. 1

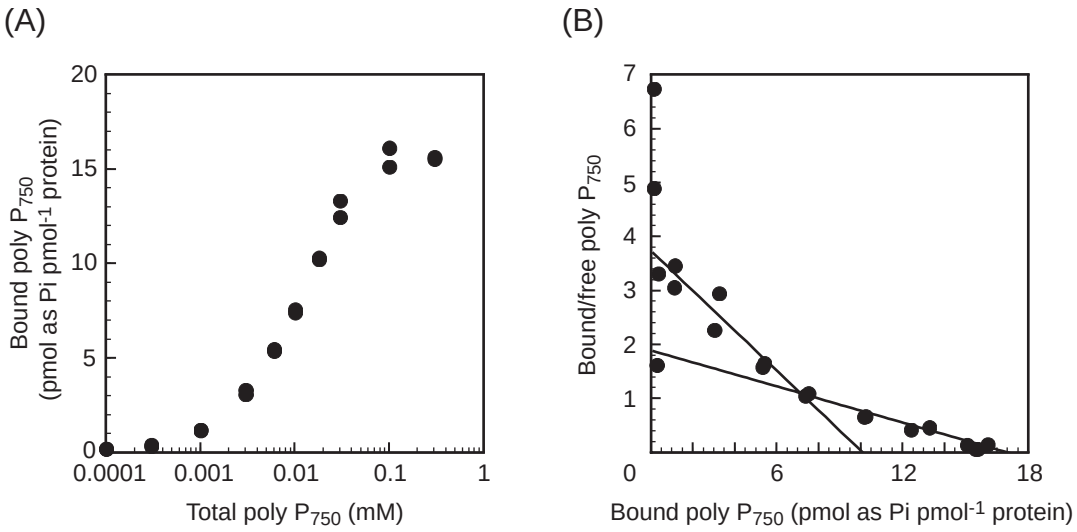
(A)
(B)
Bound poly P_{750} (pmol as Pi $pmol^{-1}$ protein)
Total poly P_{750} (mM)
Bound/free poly P_{750}
Bound poly P_{750} (pmol as Pi $pmol^{-1}$ protein)

FIG. 2

(A)

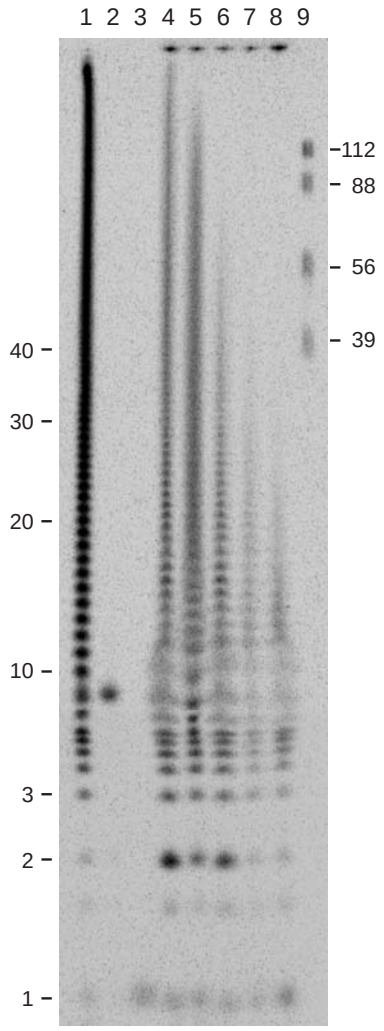
1 2 3 4 5 6 7 8 9
112
88
56
39
40
30
20
10
3
2
1

(B)

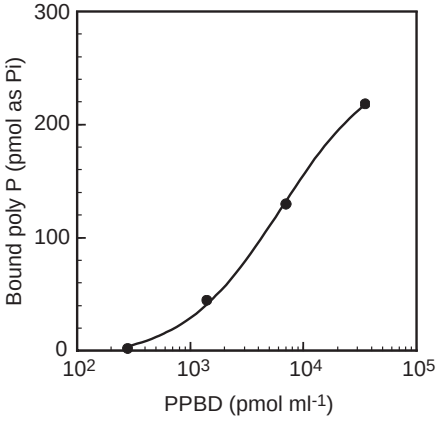
300
200
100
0
Bound poly P (pmol as Pi)
10²
10³
10⁴
10⁵
PPBD (pmol ml⁻¹)

FIG. 3

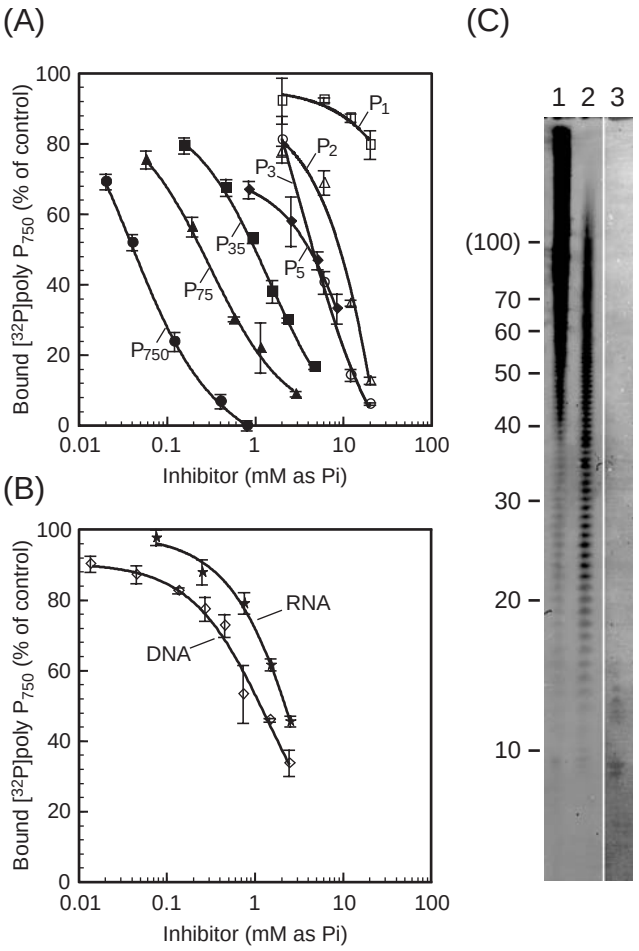
(A)
(B)
(C)
Bound [32P]poly P750 (% of control)
Inhibitor (mM as Pi)
P1
P2
P3
P5
P35
P75
P750
RNA
DNA
1 2 3
(100)
70
60
50
40
30
20
10

FIG. 4

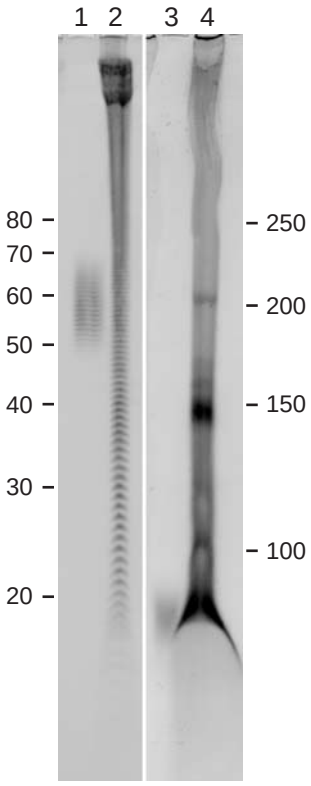

FIG. 5

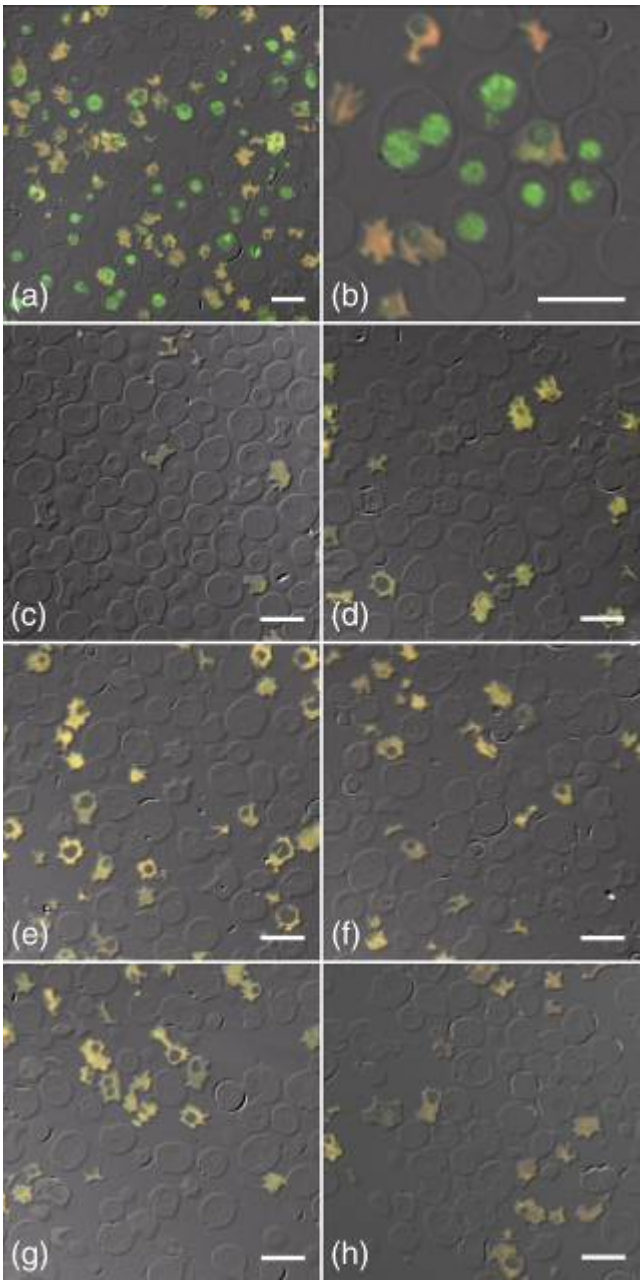

FIG. 6

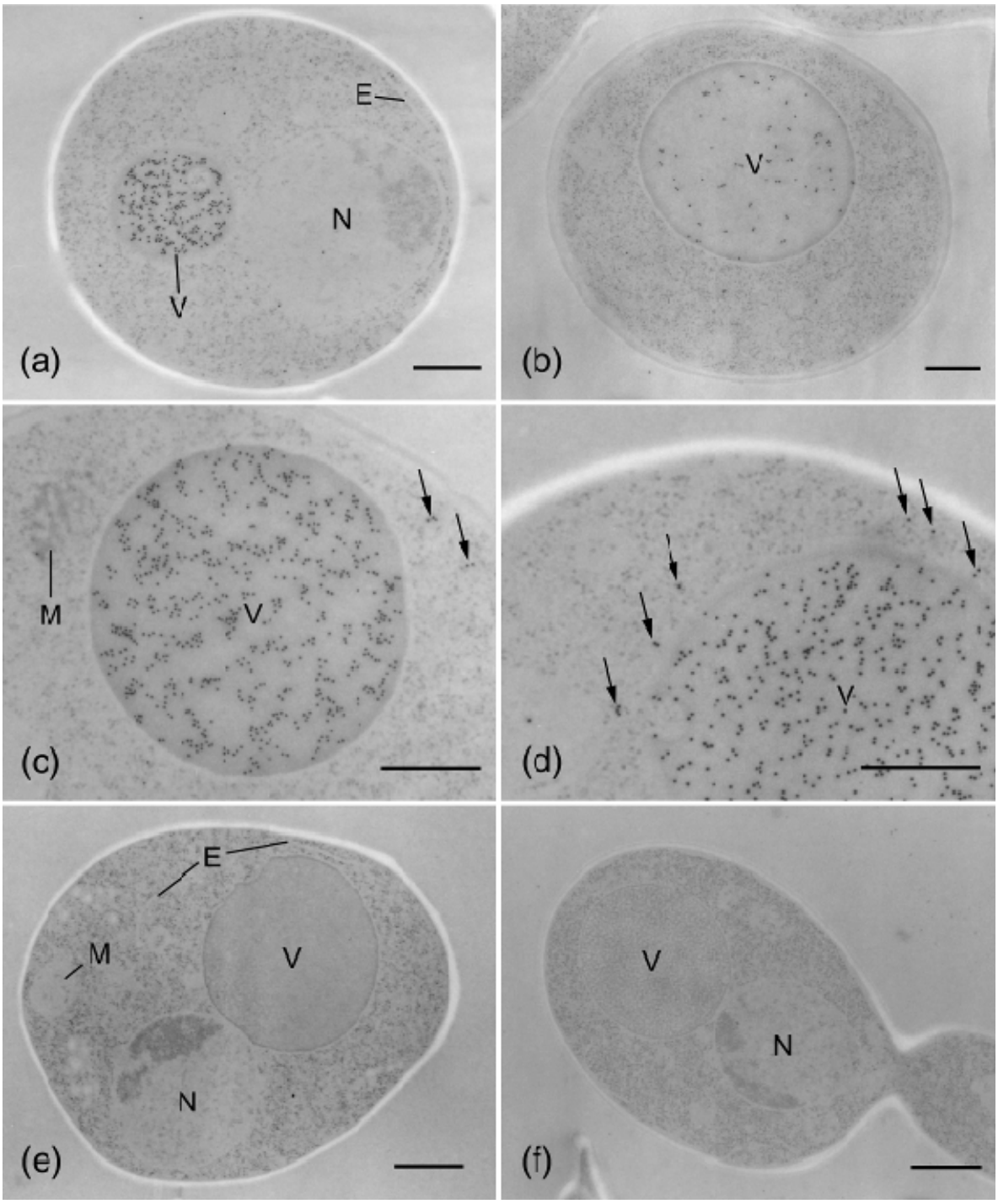

FIG. 7